Metal Ion Binding: An Electronic Structure Study of M^+(Dimethyl Ether)$_n$, M = Cu, Ag, and Au and (n = 1−4), Complexes

David Feller* and David A. Dixon

Environmental Molecular Sciences Laboratory, Pacific Northwest National Laboratory, MS K8-91, P.O. Box 999, Richland, Washington 99352

Received: October 22, 2001; In Final Form: February 12, 2002

The structures and incremental binding enthalpies of cation−ligand complexes formed from a single coinage metal cation (Cu^+, Ag^+, and Au^+) and as many as four dimethyl ether (DME) ligands are studied with second-order perturbation theory (MP2) and coupled cluster theory (CCSD(T)). Basis sets of up to augmented quintuple zeta quality were used in an effort to minimize basis set truncation error. The present results are compared with recent collision-induced dissociation measurements for the $Cu^+(DME)_n$ complexes, as well as with related complexes in which water either replaces dimethyl ether as the ligand or alkali metal cations (Li^+, Na^+, and K^+) replace the coinage metals. Agreement between the theoretical and experimental incremental binding enthalpies is good for the two larger copper complexes: $\Delta H_0(Cu^+(DME)_3) = 13.9$ (theory) vs 13.1 ± 0.9 kcal/mol (expt) and $\Delta H_0(Cu^+(DME)_4) = 11.5$ (theory) vs 10.8 ± 2.3 (expt), where values are expressed in kcal/mol. For the two smaller, more tightly bound copper complexes, the level of agreement is somewhat poorer: $\Delta H_0(Cu^+(DME)) = 48.4$ (theory) vs 44.3 ± 2.7 kcal/mol (expt) and $\Delta H_0(Cu^+(DME)_2) = 50.6$ (theory) vs 46.1 ± 1.8 (expt). In general, DME binds copper, silver, and gold 15−25% more strongly than water binds the same cations.

Introduction

Following Pederson's discovery of the class of compounds known as crown ethers in the 1960s,[1] these systems have played a key role in the field of separation science. Crown ethers are known for their ability to selectively bind specific cations in the presence of chemically similar species. Because crown ethers of practical importance are relatively large compounds by the standards of ab initio electronic structure methods, theoretical approaches to their study often involve preliminary steps which focus on smaller, prototype systems that are computationally more tractable. Such model systems provide an opportunity for calibrating less sophisticated levels of theory that are affordable for large molecules against higher accuracy, and more expensive, levels of theory. In addition, calculations on prototype systems can be essential in the development of molecular force fields because of the absence of critical experimental data.[2,3] Furthermore, gas phase experimental data, against which the results of electronic structure calculations can most easily be compared, is more likely to be available for smaller chemical systems which are easier to vaporize in a controlled manner.

Consequently, we have previously studied complexes formed from a single alkali metal cation (Li^+, Na^+, and K^+) and one or more dimethyl ether (DME) ligands, $O(CH_3)_2$.[4−6] The interaction between M^+ and DME serves as a simple model for the constituent interactions between alkali cations and oxygen-bearing crown ethers. Our calculated values of the incremental binding enthalpy, ΔH_{incr}, fell generally within 1−2 kcal/mol of collision-induced dissociation (CID) measurements.[7,8] Where larger discrepancies between theory and experiment were observed, it was difficult to identify their cause. On the theoretical side, second-order Møller−Plesset perturbation theory (MP2) calculations with the 6-31+G* basis set were the most sophisticated that could be performed at that time (1996−1997) on systems as large as $K^+(DME)_4$. On the experimental side, uncertainties arise from the need to correct the apparent onset of dissociation for the effects of multiple collisions between the cation/ether complex and the rare gas atoms. This leads to extrapolations of long tails in the cross section vs complex kinetic energy curve to the *true* energetic onset of dissociation (as opposed to the *apparent* threshold). Uncertainties may also arise from variations in the internal temperature of the complex and the finite unimolecular decay rate. The latter effect can be important because the ions move through the experimental apparatus in a relatively short period of time ($\sim 10^{-4}$ s).

Koizumi et al.[9] have recently reported experimental CID and theoretical ΔH_{incr} values for the $Cu^+(DME)_n$, n = 1−4, complexes. The two sets of values were in good agreement with each other. The theoretical values were obtained from a mixture of second and fourth order perturbation theory and density functional theory (DFT) methods, used in combination with a variety of small-to-medium size basis sets. As an illustration of the level of agreement between theory and experiment, Koizumi et al. reported theoretical values for the M^+−ether dissociation energy, $\Delta H(Cu^+(DME))$, in the range of 43.4−48.4 kcal/mol vs 44.3 ± 2.7 kcal/mol (CID/expt). For $\Delta H_{incr}(Cu^+(DME)_2)$, the theoretical values ranged from 43.6 to 50.7 kcal/mol vs 46.1 ± 1.8 kcal/mol (CID/expt.). All of the MP2 and most of the DFT theoretical binding enthalpies were corrected for the undesirable effects of basis set superposition error (BSSE). This effect, which arises from the use of incomplete basis sets, produces binding energies that are artificially stronger than would be the case in the absence of BSSE. Koizumi et al. note that restricted Hartree−Fock geometry optimizations led to highly symmetric global minimum structures of C_{2v}, D_{2d}, D_3, and S_4 for the $Cu^+(DME)_n$, n = 1−4,

* To whom correspondence should be addressed.

10.1021/jp013911j CCC: $22.00
Published on Web 04/25/2002

complexes, respectively. Optimizations at higher levels of theory found lower symmetry global minima of C_s, C_2, and C_1 symmetry for the $n = 1-3$ complexes. Because of the computational expense, no search for a lower symmetry form of $Cu^+(DME)_4$ was attempted.

In the present work, we extend our earlier studies of cation/dimethyl ether complexes to ones formed from a single coinage metal cation (Cu^+, Ag^+, and Au^+). We probe the sensitivity of the results to improvements in the one-particle (basis sets) and *n*-particle (correlation energy) spaces, the two leading causes of error in electronic structure methods. We take advantage of the development of the correlation-consistent basis sets developed in this laboratory. These basis sets provide a practical route for approaching the complete basis set limit to within a tolerance dictated by the limitation of finite computational resources. Comparisons are made with the work of Koizumi et al.[9] and with our earlier findings for $M^+(H_2O)_n$, for M a coinage metal, and $M^+(DME)_n$, where M is an alkali metal. To the best of our knowledge, no experimental or theoretical information has been reported for silver and gold complexes with DME.

Methods

The theoretical approach that was followed is similar to the approach used in our previous study of $M^+(H_2O)_n$, M = Cu, Ag, Au, complexes.[10] Preliminary MP2 geometry optimizations and normal mode calculations were performed with a combination of the diffuse function augmented 6-31+G* basis set on oxygen and the 6-31G* basis set on hydrogen and carbon.[11,12] These were paired with an [8s,6p,4d,1f] all-electron basis set for copper and similar quality relativistic effective core potential (RECP) basis sets for silver and gold. This differs somewhat from our approach for $Cu^+(H_2O)_n$ where copper was treated with an RECP. The RECP for silver was taken from the work of Andre et al.[13] and replaces a $28e^-$ core (Ar+3d). It is labeled ECP28MWB, following the Stuttgart ECP naming convention. The RECP for gold is from Schwerdtfegger et al.[14] and replaces a $60e^-$ core (Kr +4d+4f). Within the Stuttgart collection of ECPs, it is referred to as ECP60MDF. For the sake of brevity, we will refer to these relatively simple, composite basis sets by the label 6-31+G*, as indicated in Table 1.

Larger basis sets are necessary for probing the sensitivity of the predicted structures and binding enthalpies to the degree of completeness in the one-particle expansion. For H, C, and O, we used the diffuse function augmented correlation consistent basis sets, aug-cc-pVxZ, x = D − 5.[15,16] Because correlation consistent transition metal basis sets have not been reported, we used the metal basis sets developed for our study of $M^+(H_2O)_n$ complexes.[10] The aV5Z basis sets for carbon and oxygen contain two sets of *h* functions. Consequently, the corresponding copper basis set should contain multiple *i* functions for the sake of consistency. However, these were not included because of software limitations. The composition of all of the metal basis sets is given in Table 1, where we again abbreviate the aggregate basis set names to aVDZ, aVTZ, etc. Only the spherical components of the Cartesian polarization functions were used in all calculations.

Unless otherwise noted, the frozen core approximation was used for all correlated calculations; that is, the carbon and oxygen 1s pairs of electrons were excluded from the correlation treatment, along with the Ar core of copper and, of course, the core electrons included in the RECP's. Calculations were performed with Gaussian 98[17] and MOLPRO 2000[18] on an SGI Origin 2000. Large basis set (>600 functions) MP2 calculations were performed with NWChem[19] on a 512 node IBM SP.

TABLE 1: Basis Set Combinations and Cation Energies

$Cu^+(H_2O)_n$

label	Cu	$E_{MP2}(Cu^+,{}^1S)$	H,C,O
6-31+G*	[8s,6p,4d,1f]	−1638.97443	6-31+G*
aVDZ	[8s,6p,4d,1f]	−1638.97443	aug-cc-pVDZ
aVTZ	[11s,9p,5d,2f,1 g]	−1639.09578	aug-cc-pVTZ
aVQZ	[13s,12p,7d,4f,2 g,1h]	−1639.18014	aug-cc-pVQZ
aV5Z	[16s,15p,8d,5f,3 g,2h]	−1639.24640	aug-cc-pV5Z
CVTZ	[10s,7p,5d,1f]	−1793.94612	cc-pCVTZ

$Ag^+(H_2O)_n$

label	Ag	$E_{MP2}(Ag^+,{}^1S)$	H,C,O
6-31+G*/RECP[a]	[6s,5p,3d,1f]	−146.18688	6-31+G*
aVDZ/RECP	[6s,5p,3d,1f]	−146.18688	aug-cc-pVDZ
aVTZ/RECP	[8s,7p,5d,2f,1 g]	−146.50624	aug-cc-pVTZ
aVQZ/RECP	[10s,9p,7d,4f,2 g,1h]	−146.64905	aug-cc-pVQZ

$Au^+(H_2O)_n$

label	Au	$E_{MP2}(Au^+,{}^1S)$	H,C,O
6-31+G*/RECP[b]	[7s,3p,4d,1f]	−135.06768	6-31+G*
aVDZ/RECP	[7s,5p,4d,1f]	−135.06768	aug-cc-pVDZ
aVTZ/RECP	[9s,7p,6d,2f,1 g]	−135.25741	aug-cc-pVTZ
aVQZ/RECP	[11s,9p,7d,4f,2 g,1h]	−135.36233	aug-cc-pVQZ

[a] Silver core = $28e^-$ (Ar + $3d^{10}$). [b] Gold core = $60e^-$ (Kr + $4d^{10}$ + $4f^{14}$).

Geometry optimizations used the equivalent of the "tight" convergence criterion in Gaussian, which corresponds to a threshold of 1.5×10^{-5} Hartree/bohr. A complete list of Cartesian coordinates for all complexes is available from the authors upon request.

When large basis sets containing extra diffuse functions are used in molecules such as the one examined in this study, linear dependency can become a problem. In particularly severe cases, it may be impossible to converge the Hartree−Fock calculations if nothing is done to minimize the problem. Therefore, in the present work, a threshold of 10^{-5} on the eigenvalues of the overlap matrix was selected for the elimination of near linearly dependent basis functions. In practice, this threshold resulted in basis functions being removed for only the aVQZ and aV5Z basis sets. The maximum number of vectors eliminated was 15 in the case of the aV5Z basis set on Cu^+(DME). Although the removal of basis functions in the manner described above can change the total energy by several tenths of a millhartree, the effect on energy differences will be even smaller because the same threshold was used on the complex and its constituent fragments.

Vibrational frequency calculations were performed at a number of different levels of theory, as discussed below, to obtain zero-point energy corrections to the binding energies.

Results and Discussion

Copper Complexes. The MP2/aVDZ optimized structure of Cu^+(DME) possesses C_s symmetry (see Figure 1), in agreement with the calculations of Koizumi et al.[9] At this level of theory, the copper atom lies 13.6° out of the plane formed by the oxygen and two carbon atoms of DME. Forcing the copper atom back into plane results in a higher energy, higher symmetry (C_{2v}) structure that corresponds to a first-order transition state connecting the two equivalent C_s conformations. The potential energy surface for out-of-plane bending is extremely flat, as indicated by a vibrationless $C_s \rightarrow C_{2v}$ barrier height of just 0.01 kcal/mol. As the quality of the basis set improves, the out-of-plane bending angle decreases to less than 5°, suggesting that in the CBS limit it might disappear altogether. In contrast,

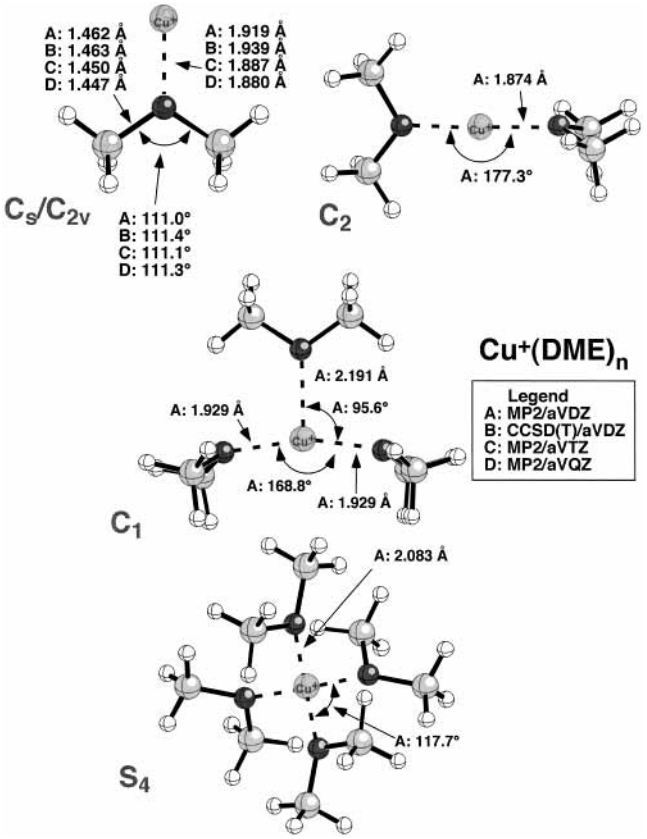

Figure 1. MP2 and CCSD(T) optimized structures for the $Cu^+(DME)_n$ complexes. The geometries for $Cu^+(DME)_n$, $n = 2-4$ were obtained at the MP2/aVDZ level of theory.

$Cu^+(H_2O)$, was predicted to have a C_{2v} structure with the same basis sets and an MP2 level of theory. Alkali metal complexes formed with DME are also found to have C_{2v} symmetry. The cause of the weak tendency for Cu^+(DME) to adopt a C_s conformation is unknown. However, we note that the barrier is so small that the complex can be considered to have C_{2v} symmetry for all practical purposes. The Cu−O bond distance in Cu^+(DME) is relatively insensitive to the quality of the basis set, contracting by 0.039 Å across the aVDZ, aVTZ, aVQZ basis set sequence (see Figure 2). At the best level of theory used in geometry optimization (MP2/aVQZ), $r_{CuO} = 1.880$ Å, a value that is slightly shorter than the corresponding distance in $Cu^+(H_2O)$, where $r_{CuO} = 1.908$ Å. This reflects the stronger metal−ligand attraction between copper and DME as discussed below.

Besides the effect of the completeness of the basis set, we have also investigated several other factors that could potentially impact the accuracy of our results. Higher order correlation contributions to the predicted Cu−O distance were determined by a series of coupled cluster theory calculations including noniterative triple excitations, CCSD(T). As shown in Table 2, CCSD(T) results in a ∼0.02 Å lengthening of r_{CuO} with the aVDZ and aVTZ basis sets. Optimization at the CCSD(T)/aVQZ level of theory proved to be computationally too expensive. Scalar relativistic effects, which are known to be important for accurate bond lengths involving transition metals, were incorporated via the mass-velocity and one-electron Darwin (MVD) corrections evaluated at the MP2/aVTZ level of theory. The former property, in atomic units, is given by

$$\frac{1}{8c^2}\sum_i p_i^4$$

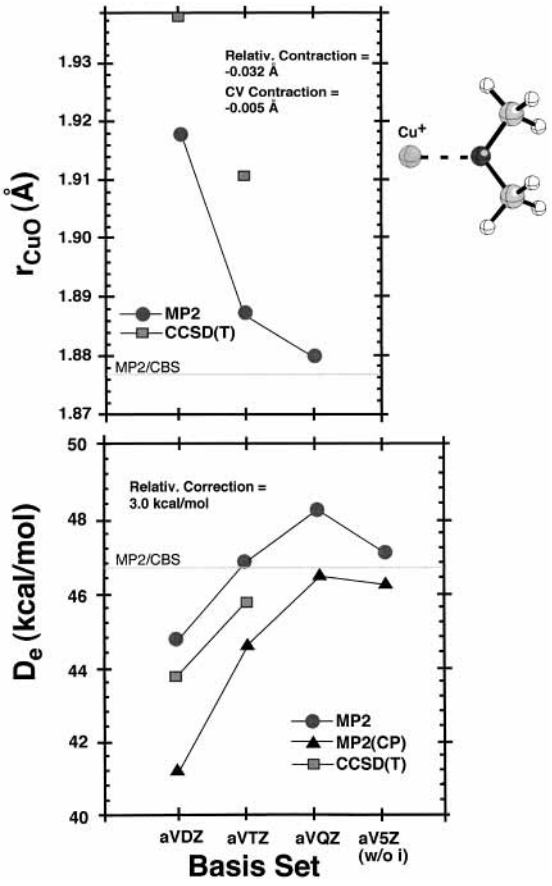

Figure 2. Convergence of the Cu−O distance and dissociation energy for Cu^+(DME) as a function of the basis set size, along with the relativistic and core/valence corrections to these properties. Counterpoise-corrected values are denoted with the suffix (CP).

and the latter by

$$\frac{\pi}{2c^2}\sum_A\sum_i Z_A\delta(r_{iA}).$$

These are the leading terms in the Breit-Pauli Hamiltonian for low Z elements. Incorporation of relativistic effects resulted in a 0.032 Å contraction of r_{CuO}, nearly canceling the lengthening associated with the use of CCSD(T).

A third and much smaller effect in this system is due to core/valence (CV) correlation. As previously noted, in conventional frozen core calculations, the carbon and oxygen 1s pair of electrons are excluded from the correlation treatment, along with the Ar core of copper. To determine the magnitude of the CV effect, we performed a series of calculations in which the carbon and oxygen 1s and the copper (3s,3p) electrons were included in the correlation treatment. The cc-pCVTZ basis set which includes additional core functions was used for DME, and a modified [13s,10p,6d,2f,1g] contracted basis set with additional "tight" functions to better represent the core was used for copper. The MP2(CV) calculations predicted a 0.005 Å shortening of the Cu−O distance. For the larger $Cu^+(DME)_n$ complexes, where geometry optimization with extended basis sets, higher order correlation, scalar relativistic corrections, and CV correlation was too expensive, we expect that the MP2/aVDZ level of theory should yield copper-ligand distances that are ∼0.05 Å too long, based on our calculations for Cu^+(DME).

Zero-point exclusive, electronic dissociation energies (D_e) for Cu^+(DME) at the MP2 and CCSD(T) levels of theory are listed in Table 2 and are depicted graphically in Figure 2 as a function

TABLE 2: $Cu^+(DME)_n$ Total Energies (E_h), Optimized Cu−O Bond Lengths (Å), and Vibrationless, Incremental Electronic Dissociation Energies, D_e(kcal/mol)

system	basis	# funct's	method	total energy	r_{CuO}	r_{CuO}'	D_e
$Cu^+(DME)$ (C_s/C_{2v})[a]	aVDZ	176	MP2	−1793.63716	1.919		44.6
			CCSD(T)	−1793.64675	1.939		43.8
	aVTZ	362	MP2	−1793.90887	1.887		47.2
			CCSD(T)	−1793.91228	1.911		45.9
	aVQZ	657	MP2	−1794.04046	1.880		48.5
	aV5Z[b]	1046	MP2	−1794.12063	1.880		47.1
$Cu^+(DME)_2$ (C_2)	aVDZ	299	MP2	−1948.30247	1.874		46.3
			CCSD(T)	−1948.36269			44.2
	aVTZ[c]	638	MP2	−1948.72284			48.8
	aVQZ[c]	1173	MP2	−1948.90006			49.4
$Cu^+(DME)_3$ (C_1)	aVDZ	422	MP2	−2102.92203	2.191	1.929	17.5
	aVTZ[c]	914	MP2	−2103.48644			16.6
	aVQZ[c]	1689	MP2	−2103.70726			15.8
$Cu^+(DME)_4$ (S_4)	aVDZ	545	MP2	−2257.53795	2.083		15.3
	aVTZ[c]	1190	MP2	−2258.24559			13.8

[a] At the MP2/aVDZ level of theory, the optimized structure has C_s symmetry. At the MP2/aVTZ and MP2/aVQZ levels of theory, the structure was within 5° of C_{2v}. [b] Calculation performed at the optimal MP2/aVQZ geometry. [c] Calculation performed at the optimal MP2/aVDZ geometry.

of the basis set size. The convergence pattern is similar to that observed for $Cu^+(H_2O)$ with the same basis sets. After increasing almost linearly from aVDZ through aVQZ, the binding energy decreases by 1.4 kcal/mol to 47.1 kcal/mol with the large aV5Z basis set. This failure to exhibit monotonic convergence probably reflects some residual underlying irregularity in the copper basis sets. Similar energetic effects with respect to the complete basis set limit have been observed for other hydrogen bonded systems as a function of the correlation consistent basis sets.[20]

Theoretical binding energies are often corrected for the artificial effects of BSSE by applying the counterpoise correction (CP) of Boys and Bernardi.[21] However, our experience with a variety of cation/ligand complexes and the diffuse function augmented correlation consistent basis sets indicates that CP-corrected binding energies often differ more from the complete basis set limit than the raw values.[10,22,23] As shown in Figure 2, the situation with $Cu^+(DME)$ is more complicated. For the aVDZ and aVTZ basis sets, the CP corrections are substantial, and their inclusion results in binding energies that seriously underestimate the CBS limit, taken as the average of the aV5Z and CP-corrected aV5Z values. However, for the aVQZ basis sets, the CP corrected binding energy is closer to the CBS limit than the raw, uncorrected value. Ultimately, of course, the raw and CP-corrected results must converge to the same limit. Based on these findings for $Cu^+(DME)$, we adopt the CP-corrected values as our best estimate of the CBS limit for $Cu^+(DME)_2$ and $Cu^+(DME)_3$. For $Cu^+(DME)_4$, where the aVTZ basis set was the largest set that could be afforded, we adopt the raw result as our best binding energy.

The theoretical binding enthalpy of $Cu^+(DME)$ at 0 K (ΔH_0) is listed in Table 3 along with the contributions to it from zero-point energy (ΔE_{ZPE}), scalar relativistic effects (ΔE_{SR}), higher order correlation ($\Delta E_{CCSD(T)}$), and core/valence correlation (ΔE_{CV}). The levels of theory at which the various terms were calculated are given in the table. Of the latter three, the scalar relativistic correction is seen to be the largest at 3.2 kcal/mol (evaluated at the MP2/aVTZ+rel. geometry, r_{CuO} = 1.855 Å) and acts to increase the binding energy. ΔE_{SR} is relatively insensitive to the copper−oxygen distance, dropping by only 0.2 kcal/mol at the longer MP2/aVTZ bond length of r_{CuO} = 1.887 Å. Some measure of the accuracy of the MP2/aVTZ relativistic correction can be found in a small calibration study on the $Cu^+(H_2O)$ complex, where four-component relativistic MP2 and CCSD(T) fell within 0.3 kcal/mol of the MVD/aVTZ values.[10] The higher order correlation correction based on the CCSD(T) energies is negative, leading to a decrease in the binding energy, whereas the core/valence correction is positive and slightly smaller than the $\Delta E_{CCSD(T)}$ value, so that they partially cancel each other.

TABLE 3: $Cu^+(DME)_n$ Incremental Binding Enthalpies[a]

$Cu^+(DME)$		comments
best MP2(FC) D_e	46.9	MP2(FC)/aV5Z[c]
ΔE_{ZPE}	−1.1	MP2(FC)/aVDZ
ΔE_{SR}	3.2	MP2(FC)/aVTZ
$\Delta E_{CCSD(T)}$	−1.3	CCSD(T)(FC)/aVTZ
ΔE_{CV}	0.7	MP2/CVTZ
total	48.4	
expt[b]	44.3 ± 2.7	
$Cu^+(DME)_2$		comments
best MP2(FC) D_e	48.7	MP2(FC)/aVQZ[d]
ΔE_{ZPE}	−1.6	MP2/6-31+G*
ΔE_{SR}	4.4	MP2/aVDZ
$\Delta E_{CCSD(T)}$	−2.0	CCSD(T)/aVDZ
ΔE_{CV}	1.2	MP2/CVDZ
total	50.6	
expt[b]	46.1 ± 1.8	
$Cu^+(DME)_3$		comments
best MP2(FC) D_e	15.8	MP2/aVQZ[d]
ΔE_{ZPE}	−0.7	MP2/6-31+G*
ΔE_{SR}	−1.2	RHF/aVDZ
total	13.9	
expt[b]	13.1 ± 0.9	
$Cu^+(DME)_4$		comments
best MP2(FC) D_e	13.8	MP2/aVTZ
ΔE_{ZPE}	−0.9	MP2/6-31+G*
ΔE_{SR}	−1.4	RHF/aVDZ
total	11.5	
expt[b]	10.8 ± 2.3	

[a] ZPE = zero point energy, CV = core/valence correction, and SR = scalar relativistic correction. Basis set definitions are given in Table 1. [b] Koizumi et al., ref 9. [c] Average of the raw and counterpoise-corrected aV5Z binding energies. [d] Average of the raw and counterpoise-corrected aVQZ binding energies.

The final theoretical value of $\Delta H_0(Cu^+(DME))$ is 48.4 kcal/mol, which lies somewhat outside the CID/expt. range of 44.4 ± 2.7 kcal/mol reported by Koizumi et al.[9] When the same theoretical approach was applied in the case of $Cu^+(H_2O)$,[10] it produced a binding enthalpy of 39.0 kcal/mol, compared to experimental measurements of 36 ± 3[24] and 38.4 ± 1.4 kcal/mol.[25] The latter value is from the Armentrout group, the same group responsible for the most recent experimental work on

$Cu^+(DME)_n$ complexes.[9] Our calculated value lies at the top end of the range of theoretical values (43.4 to 48.4 kcal/mol) given by Koizumi et al. We note that they used smaller basis sets than employed in this work, and as shown in Figure 2, the binding energy does exhibit a dependence on the quality of the basis set, with smaller basis sets giving smaller binding energies. In addition, Koizumi et al. performed an MP4 calculation with a basis set similar to the aVDZ basis set and obtained D_e = 48.8 kcal/mol, as compared to our CCSD(T)/aVDZ value of 43.8 kcal/mol and our CCSD(T)/aVTZ value of 45.9 kcal/mol. Koizumi et al. report an MP2 value of D_e = 45.1 kcal/mol using the same basis set as was used in their MP4 calculation. This increase in binding energy for MP4 vs MP2 is exactly opposite to the trend that we find with our MP2 and CCSD(T) calculations. Koizumi et al. briefly discuss the potential convergence problems in the MPn sequence. These results further show that the binding energy is sensitive to both the basis set and correlation treatment. The inclusion of scalar relativistic and core/valence corrections in the present work are also potential sources of difference between the present ΔH_0 and previously reported theoretical values. We also note that our ΔE_{ZPE} correction is smaller than the value of Koizumi et al. by ~0.3 kcal/mol.

The $Cu^+(DME)_2$ complex exhibits C_2 symmetry with two equivalent Cu−O bonds that are 0.045 Å *shorter* than the Cu−O bond in Cu^+(DME). As suggested by this contraction in bond lengths, the $Cu^+(DME)_2 \rightarrow Cu^+(DME)$ + DME incremental binding enthalpy listed in Table 3 represents an *increase* of ~3 kcal/mol over the $Cu^+(DME) \rightarrow Cu^+$ + DME dissociation energy. Contributing to this increase is an electronic binding energy that is 1.7 kcal/mol stronger and ΔE_{ZPE}, ΔE_{SR}, $\Delta E_{CCSD(T)}$, and ΔE_{CV} corrections that are all larger for $Cu^+(DME)_2$ than Cu^+(DME). ΔE_{SR} now represents almost 10% of the electronic binding energy. The increase in binding enthalpy observed for $Cu^+(DME)_2$ stands in stark contrast to the binding pattern for the corresponding alkali metal complexes, where a monotonic decrease in binding strength is observed as each additional DME ligand expands the complex. This anomalously large binding enthalpy for the second ligand has been rationalized in the case of $Cu^+(H_2O)_2$ by Bauschlicher and co-workers.[26−28] Their explanation is based on copper sd_σ hybridization which, it is argued, can reduce the metal−ligand repulsion when two oxygens are situated collinearly across the cation from each other.

Compared with Cu^+(DME), the agreement between theory and experiment is somewhat poorer for $Cu^+(DME)_2$. The CID/expt ΔH_0 value is smaller than the theoretical estimate by more than 5 kcal/mol, 50.6 kcal/mol (theory) vs 46.1 ± 1.8 kcal/mol (expt). It is difficult to know how to interpret the difference between theory and experiment. Essentially the same theoretical approach was used in our earlier copper/water study, where the $Cu^+(H_2O)_2$ incremental binding enthalpy, 43.8 kcal/mol (theory), was only slightly outside the error bars of the only available experimental values (40 ± 3[24] and 40.7 ± 1.6[25] kcal/mol). Additionally, the agreement for $Cu^+(H_2O)$ was very good, 39.0 (theory) vs 38.4 ± 1.4 kcal/mol (expt).[25] The difference in the binding energy of the first and second DME is 1.8 kcal/mol (expt) vs 2.9 kcal/mol (theory), with both approaches in agreement that the second binding energy is larger. A comparison with the theoretical results of Koizumi et al.[9] shows that, regardless of the basis set, the DFT methods failed to predict an increase in binding energy for the second ligand. Only the fourth order perturbation theory (MP4) value with the large hybrid basis set (similar to our aVDZ basis set as noted above) predicts a change in ΔH_0 that is in good agreement with the present results.

MP2/aVDZ optimizations produced a T-shaped, C_1 symmetry conformation for $Cu^+(DME)_3$, in agreement with the MP2 and DFT calculations of Koizumi et al. (see Figure 1). The unique Cu−O bond at 2.191 Å is more than 0.26 Å longer than the two Cu−O bonds. Qualitatively, this means that the third DME binds much more weakly than the first or second ligand. The excellent agreement between the incremental binding enthalpies in Table 3, 13.9 kcal/mol (theory) vs 13.1 ± 0.9 kcal/mol (expt), may be partially fortuitous. Because of the prohibitive computational expense, it was not possible to determine the ΔE_{CV} and $\Delta E_{CCSD(T)}$ corrections to the binding energy. Although we would expect them to approximately cancel, as found for Cu^+(DME) and $Cu^+(DME)_2$, the net correction may still be on the order of 0.5 kcal/mol. One factor that suggests the net correction may be smaller than this is the small size of $\Delta H_0(Cu^+(DME)_3)$ and ΔE_{SR}, which is now much smaller and of opposite sign to the two previous complexes. Compared to the third water ligand in $Cu^+(H_2O)_3$, the third DME ligand binds ~20% less strongly.

Only one $Cu^+(DME)_4$ conformation was identified. It possessed S_4 symmetry, with a Cu−O distance of 2.083 Å, slightly longer than the average of the distances in $Cu^+(DME)_3$. A normal-mode analysis verified that the structure was a minimum on the restricted Hartree−Fock (RHF)/6-31+G* potential energy surface. Attempts to locate a structure of lower symmetry at the MP2/6-31+G* level of theory were unsuccessful. The computed incremental binding enthalpy of the fourth ligand (11.5 kcal/mol) was 2.4 kcal/mol less than the binding enthalpy of the third DME, in almost exact agreement with the 2.3 kcal/mol measured in the CID experiment. The range of the experimental binding enthalpy (10.8 ± 2.3 kcal/mol) easily encompasses the theoretical value. Unlike the smaller complexes, where basis sets as large as aVQZ could be used, for $Cu^+(DME)_4$, it proved prohibitively expensive to perform an MP2/aVQZ calculation. In light of the aVDZ → aVTZ trend in D_e to smaller values for the trimer and tetramer, the aVQZ basis set would probably yield a somewhat smaller value of D_e by 0.5−1.0 kcal/mol based on the trimer results. For comparison purposes, the binding enthalpies of all four $Cu^+(DME)_n$ complexes are compared to experiment in Figure 3.

Koizumi et al.[9] identified several alternative conformations of $Cu^+(DME)_3$ and $Cu^+(DME)_4$ at the MP2/3-21G level of theory that differed from the structures examined here in that one or more ligands were bound to the complex via DME hydrogen bonds, rather than directly to the metal cation. We have previously shown[10] for $Cu^+(H_2O)_3$ and $Cu^+(H_2O)_4$ that the lowest energy conformations were of the (2,1) and (2,2) variety, where the notation (*m*,*n*) indicates the presence of *m* dimethyl ethers bound to the metal and *n* dimethyl ethers in the second shell, bound by hydrogen bonds to the first shell. MP2/aVDZ calculations predict the $(DME)_2$ dimer to be a weakly bound complex with C_{2h} symmetry (see Figure 4). The computed binding energy of ~1.9 kcal/mol per C−H···O hydrogen bond compares with a value of 5.0 kcal/mol for a OH···H hydrogen bond in $(H_2O)_2$[29] and is consistent with the energies of other C−H O hydrogen bonds.[30,20] Because this is significantly weaker than the incremental binding energies already discussed, no attempt was made to pursue such higher energy conformations.

Silver and Gold Complexes. Optimized M−O distances and D_e values for the eight complexes formed with silver and gold are listed in Table 4. As was the case with Cu^+(DME), the Ag^+(DME) and Au^+(DME) complexes possess C_s symmetry,

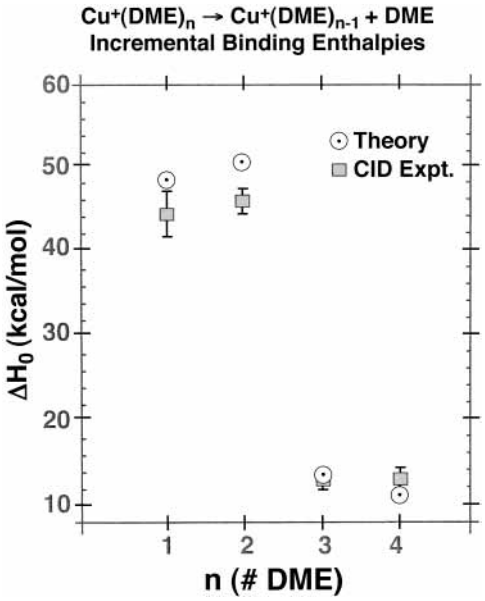

Figure 3. Comparison of theoretical and experimental binding enthalpies for the $Cu^+(DME)_n$ complexes. Optimized $(DME)_2$ and $(H_2O)_2$ structures and Mulliken partial charges. MP2/aVDZ optimized structure for $Au^+(DME)_4$.

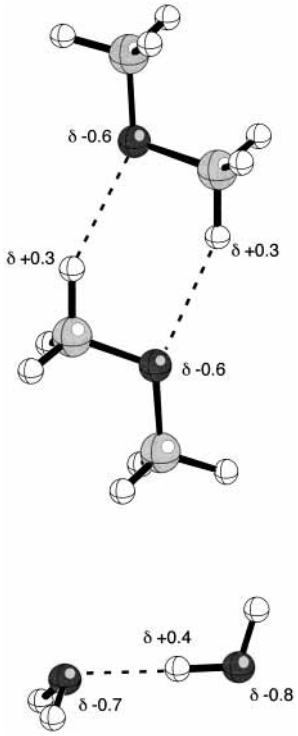

Figure 4. Optimized $(DME)_2$ and $(H_2O)_2$ structures and Mulliken partial charges.

and the out-of-plane bend angle of the cation decreases significantly as the geometry optimization is carried out with larger and larger basis sets. For comparison, $Ag^+(H_2O)$ and $Au^+(H_2O)$ possess C_{2v} and C_s symmetry, respectively, with very soft potentials for out-of-plane bending. Even the strongly bound H_3O^+ ion, with a 0 K binding energy of 163.7 kcal/mol,[31] has a very flat inversion potential with a low barrier to inversion.[32]

Unlike their alkali cation/DME counterparts, which display monotonic trends in r_{MO} (which lengthen) and D_e (which decrease) as a function of increasing atomic number, the trends across the $Cu^+(DME)$, $Ag^+(DME)$ and $Au^+(DME)$ sequence are less regular. In this regard, they more closely follow the trends observed for $M^+(H_2O)$, M= Cu, Ag, and Au, where $Au^+(H_2O)$ exhibits a shorter than expected metal−water distance and a binding energy that is larger than that for the silver complex. Pyykkö[33] coined the phrase "gold anomaly" to describe that element's deviation from alkali cation-like behavior when forming complexes. In addition, it is well-established that the metal−metal binding energy in Ag clusters is less than the Cu and Au values even for the diatomics and that the Cu and Au values tend to be closer to each other.[34] The electronic binding energy of $Au^+(DME)$ is 15.1 kcal/mol stronger than the binding in $Ag^+(DME)$ and 7.1 kcal/mol more than in $Cu^+(DME)$. By comparison, the corresponding differences with water as the ligand are 10.0 (Au^+ vs Ag^+) and 1.1 kcal/mol (Au^+ vs Cu^+), with $Au^+(H_2O)$ being the most strongly bound in all cases.

Binding enthalpies at 0 K, including corrections for higher order correlation recovery via CCSD(T) and limited core/valence effects, are provided in Table 5. Although no experimental measurements have been reported for $Ag^+(DME)$, the same theoretical treatment in $Ag^+(H_2O)$ yielded good agreement, 31.9 kcal/mol (theory) vs 33.3 ± 2.2 kcal/mol (expt).[35] The second DME ligand binds slightly less strongly to silver, counter to what was found for copper and gold. For $Au^+(DME)_2$, the excess binding of the second ligand is ∼5 kcal/mol more than the first, whereas for $Cu^+(DME)_2$, this difference was only 2.9 kcal/mol. For Ag^+, there is essentially no difference between the first and second binding energies. The binding energy of the third ligand is markedly smaller than that of the first or second for all three metals. However, the difference is most dramatic for gold, falling by a factor of more than five, compared to the second binding energy.

$Cu^+(DME)_4$ and $Ag^+(DME)_4$ complexes adopted an S_4 high symmetry conformation. However, the S_4 optimized geometry of $Au^+(DME)_4$ possesses three small imaginary frequencies (11.1i, 11.1i, and 6.2i cm^{-1}) at the RHF/6-31+G* level of theory. By following the directions associated with the imaginary frequencies downhill, a C_1 structure was identified on the potential energy surface that was 0.8 kcal/mol lower in energy. Although it was prohibitively expensive to perform a normal-mode analysis at the MP2 level of theory with any of the correlation consistent basis sets, experience with the $M^+(H_2O)_n$ complexes suggests that the precise characterization of high symmetry vs low symmetry structures on the potential surface may be quite sensitive to the theoretical treatment.

The final $Au^+(DME)_4$ structure can be seen in Figure 5 to resemble the $Au^+(DME)_2$ complex with two additional, loosely bound ligands. This finding, together with the binding pattern observed for the first and second ligand, suggests that, although the electronic interactions are stronger for gold, the size effect dominates for the additional two ligands, resulting in weaker binding than was seen in the corresponding Ag or Cu complexes. For all three metals, the fourth ligand is bound nearly as strongly as the third. In the case of silver, the difference is just 0.4 kcal/mol. Silver also showed very little difference between the first and second ligands. The third and fourth binding energies are strongest for Ag^+ followed by Cu^+ and then Au^+, exactly opposite to the trends for the first two binding energies.

Conclusions

Second-order perturbation theory and coupled cluster theory calculations were performed with large all-electron and RECP basis sets on the $M^+(DME)_n$ ionic complexes, M = Cu, Ag, and Au and $n = 1-4$, to determine optimized structures and incremental binding enthalpies. This is the first report, either experimental or theoretical, dealing with the silver and gold

TABLE 4: $Ag^+(DME)_n$ and $Au^+(DME)_n$ Total Energies (E_h), Optimized M−O Bond Lengths (Å) and Vibrationless, Incremental Dissociation Energies, D_e (kcal/mol)

system	basis	# funct's	method	total energy	r_{AgO}	r_{AgO}'	D_e
$Ag^+(DME)$ (C_s)	aVDZ	166	MP2	−300.83978	2.147		38.5
			CCSD(T)	−300.88776	2.164		37.5
	aVTZ	349	MP2	−301.30564	2.125		38.6
			CCSD(T)[b]	−301.30482			36.8
	aVQZ	645	MP2	−301.49448	2.123		39.1
$Ag^+(DME)_2$ (C_2)	aVDZ	289	MP2	−455.49231	2.104		38.2
	aVTZ[a]	629	MP2	−456.10183			37.5
	aVQZ[a]	1161	MP2	−456.33592			37.8
$Ag^+(DME)_3$ (C_1)	aVDZ	412	MP2	−610.11671	2.192	2.284	20.6
	aVTZ[a]	905	MP2	−610.86627			16.7
$Ag^+(DME)_4$ (S_4)	aVDZ	535	MP2	−764.74111	2.281		20.6
	aVTZ[a]	1181	MP2	−765.62953			16.3
system	basis	# funct's	method	energy	r_{AuO}	r_{AuO}'	D_e
$Au^+(DME)$ (C_s)	aVDZ	172	MP2	−289.73866	2.055		49.8
			CCSD(T)	−289.77282	2.089		47.9
	aVTZ	359	MP2	−290.08073	2.019		53.6
			CCSD(T)[b]	−290.12331			50.7
	aVQZ	647	MP2	−290.23178	2.013		54.2
$Au^+(DME)_2$ (C_2)	aVDZ	295	MP2	−444.42569	2.009		59.9
	aVTZ[a]	635	MP2	−444.91614			61.6
	aVQZ[a]	1163	MP2	−451.11190			62.3
$Au^+(DME)_3$ (C_1)	aVDZ	418	MP2	−599.03949	2.016	2.829	13.9
	aVTZ[a]	911	MP2	−599.67273			12.2
$Au^+(DME)_4$ (C_1)	aVDZ	541	MP2	−753.65038	2.027	2.789	12.1
	aVTZ[a]	1187	MP2	−754.42636			10.3

[a] Calculation performed at the optimal MP2/aVDZ geometry. [b] Calculation performed at the optimal MP2/aVTZ geometry.

TABLE 5: $Ag^+(DME)_n$ and $Au^+(DME)_n$ Incremental Binding Enthalpies, ΔH_0[a]

system	ΔH_0	system	ΔH_0
$Ag^+(DME)$		**$Au^+(DME)$**	
best MP2(FC) D_e	39.1	best MP2(FC) D_e	54.2
ΔE_{ZPE}	−0.7	ΔE_{ZPE}	−1.0
$\Delta E_{CCSD(T)}$	−1.8	$\Delta E_{CCSD(T)}$	−2.9
total ΔH_0	36.6	total ΔH_0	50.3
$Ag^+(DME)_2$		**$Au^+(DME)_2$**	
best MP2(FC) D_e	37.8	best MP2(FC) D_e	62.2
ΔE_{ZPE}	−1.1	ΔE_{ZPE}	−1.8
$\Delta E_{CCSD(T)}$	−0.6	$\Delta E_{CCSD(T)}$	−5.0
total ΔH_0	36.7		60.4
$Ag^+(DME)_3$		**$Au^+(DME)_3$**	
best MP2(FC) D_e	16.6	best MP2(FC) D_e	12.2
ΔE_{ZPE}	−0.4	ΔE_{ZPE}	−0.5
total ΔH_0	16.2	total ΔH_0	11.7
$Ag^+(DME)_4$		**$Au^+(DME)_4$**	
best MP2(FC) D_e	16.3	best MP2(FC) D_e	10.3
ΔE_{ZPE}	−0.5	ΔE_{ZPE}	−0.5
total ΔH_0	15.8	total ΔH_0	9.8

[a] ZPE = zero point energy. Basis set definitions are given in Table 1.

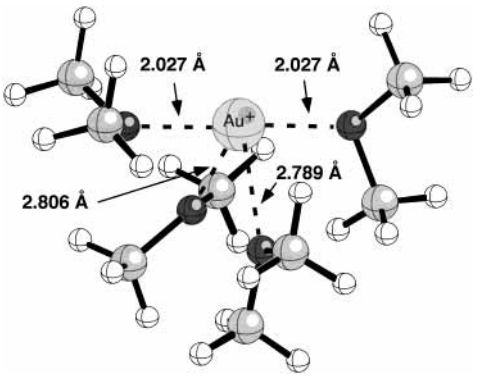

Figure 5. MP2/aVDZ optimized structure for $Au^+(DME)_4$.

complexes. Although second-order perturbation theory is capable of semiquantitative accuracy in predicting binding enthalpies for these systems, corrections for relativistic effects, higher order correlation and core/valence correlation effects can all contribute on the order of 1−4 kcal/mol.

Agreement between theory and experiment for the copper complexes, the only ones for which experimental data is available, was within the experimental error bars for $n = 3$ and 4, but the calculations overestimate the experimental values for $n = 1$ and 2. In the worse case, $Cu^+(DME)_2$, the difference was as large as 5.2 ± 1.8 kcal/mol. If an additional correction for basis set completeness is estimated for $Cu^+(DME)_2$, the difference in the binding energies for $n = 1$ and 2 are comparable, both ∼4 kcal/mol. In contrast, for the analogous copper/water complexes, theory was within both quoted experimental error bars for the $n = 1$ case and was slightly higher than experiment for the $n = 2$ case. Thus, because basically the same theoretical approach was used to study the copper/water complexes as was used here, the reason for the relatively large difference between theory and experiment for $Cu^+(DME)$ and $Cu^+(DME)_2$ remains unclear.

Acknowledgment. Dr. Michel Dupuis is thanked for a critical reading of the manuscript prior to publication. Dr. Peter Armentrout is thanked for early access to his group's experimental results. This research was supported, in part, by the U.S. Department of Energy, Office of Basis Energy Research, Chemical Sciences, and Office of Biological and Environmental Research, under Contract No. DE-AC06-76RLO 1830. This research was performed, in part, using the Molecular Science Computing Facility (MSCF) in the William R. Wiley Environmental Molecular Sciences Laboratory at the Pacific Northwest National Laboratory. The MSCF is a national user facility funded by the Office of Biological and Environmental Research in the U.S. Department of Energy. The Pacific Northwest National Laboratory is a multiprogram national laboratory operated by Battelle Memorial Institute.

References and Notes

(1) Pedersen, C. J. *J. Am. Chem. Soc.* **1967**, *89*, 2495.
(2) Hay, B. P.; Rustad, J. R.; Hostetler, C. J. *J. Am. Chem. Soc.* **1993**, *115*, 11158.
(3) Hay, B. P.; Rustad, J. R. *J. Am. Chem. Soc.* **1994**, *116*, 6316.
(4) More, M. B.; Glendening, E. D.; Ray, D.; Feller, D.; Armentrout, P. B. *J. Phys. Chem.* **1996**, *100*, 1605.
(5) Feller, D.; Aprà, E.; Nichols, J. A.; Bernholdt, D. E. *J. Chem. Phys.* **1996**, *105*, 1940.
(6) Hill, S. E.; Glendening, E. D.; Feller, D. *J. Phys. Chem.* **1997**, *101*, 6125.
(7) More, M. B.; Ray, D.; Armentrout, P. B. *J. Phys. Chem. A* **1996**, *101*, 831.
(8) More, M. B.; Ray, D.; Armentrout, P. B. *J. Phys. Chem. A* **1997**, *101*, 4254.
(9) Koizumi, H.; Zhang, X.; Armentrout, P. B. *J. Phys. Chem.* **2001**, *105*, 2444.
(10) Feller, D.; Glendening, E. D.; deJong, W. A. *J. Chem. Phys.* **1999**, *110*, 1475.
(11) Hehre, W. J.; Ditchfield, R.; Pople, J. A. *J. Chem. Phys.* **1972**, *56*, 2257.
(12) Hariharan, P. C.; Pople, J. A. *Theor. Chim. Acta* **1973**, *28*, 213.
(13) Andrae, D.; Haeussermann, U.; Dolg, M.; Stoll, H.; Preuss, H. *Theor. Chim. Acta* **1990**, *77*, 123.
(14) Schwerdtfegger, P.; Dolg, M.; Schwarz, W. H. E.; Bowmaker, G. A.; Boyd, P. D. W. *J. Chem. Phys.* **1989**, *91*, 1762.
(15) Dunning, T. H., Jr. *J. Chem. Phys.* **1989**, *90*, 1007.
(16) Kendall, R. A.; Dunning, T. H., Jr.; Harrison, R. J. *J. Chem. Phys.* **1992**, *96*, 6796.
(17) Frisch, M. J.; Trucks, G. W.; Schlegel, H. B.; Scuseria, G. E.; Robb, M. A.; Cheeseman, J. R.; Zakrzewski, V. G.; Montgomery, J. A., Jr.; Stratmann, R. E.; Burant, J. C.; Dapprich, S.; Millam, J. M.; Daniels, A. D.; Kudin, K. N.; Strain, M. C.; Farkas, O.; Tomasi, J.; Barone, V.; Cossi, M.; Cammi, R.; Mennucci, B.; Pomelli, C.; Adamo, C.; Clifford, S.; Ochterski, J.; Petersson, G. A.; Ayala, P. Y.; Cui, Q.; Morokuma, K.; Malick, D. K.; Rabuck, A. D.; Raghavachari, K.; Foresman, J. B.; Cioslowski, J.; Ortiz, J. V.; Stefanov, B. B.; Liu, G.; Liashenko, A.; Piskorz, P.; Komaromi, I.; Gomperts, R.; Martin, R. L.; Fox, D. J.; Keith, T.; Al-Laham, M. A.; Peng, C. Y.; Nanayakkara, A.; Gonzalez, C.; Challacombe, M.; Gill, P. M. W.; Johnson, B. G.; Chen, W.; Wong, M. W.; Andres, J. L.; Head-Gordon, M.; Replogle, E. S.; Pople, J. A. *Gaussian 98*, revision A.7; Gaussian, Inc.: Pittsburgh, PA, 1998.
(18) Werner, H.-J.; Knowles, P. J.; Amos, R. D.; Bernhardsson, A.; Berning, A.; Celani, P.; Cooper, D. L.; Deegan, M. J. O.; Dobbyn, A. J.; Eckert, F.; Hampel, C.; Hetzer, G.; Korona, T.; Lindh, R.; Lloyd, A. W.; McNicholas, S. J.; Manby, F. R.; Meyer, W.; Mura, M. E.; Nicklass, A.; Palmieri, P.; Pitzer, R. M.; Rauhut, G.; Schütz, M.; Stoll, H.; Stone, A. J.; Tarroni, R.; Thorsteinsson, T. *MOLPRO 2000*; Universitat Stuttgart: Stuttgart, Germany, 2000.
(19) Anchell, J.; Apra, E.; Bernholdt, D.; Borowski, P.; Bylaska, E.; Clark, T.; Clerc, D.; Dachsel, H.; de Jong, B.; Deegan, M.; Dupuis, M.; Dyall, K.; Elwood, D.; Fann, G.; Fruchtl, H.; Glendening, E. D.; Gutowski, M.; Harrison, R.; Hess, A.; Jaffe, J.; Johnson, B.; Ju, J.; Kendall, R.; Kobayashi, R.; Kutteh, R.; Lin, Z.; Littlefield, R.; Long, X.; Meng, B.; Nichols, J.; Nieplocha, J.; Rendall, A.; Rosing, M.; Sandrone, G.; Stave, M.; Straatsma, T.; Taylor, H.; Thomas, G.; van Lenthe, J.; Windus, T.; Wolinski, K.; Wong, A.; Zhang, Z. *NWChem*; Pacific Northwest National Laboratory: Richland, WA, 1999.
(20) Vargas, R.; Garza, J.; Freisner, R. A.; Stern, H.; Hay, B. P.; Dixon, D. A. *J. Phys. Chem. A* **2001**, *105*, 4963.
(21) Boys, S. F.; Bernardi, F. *Mol. Phys.* **1970**, *19*, 553.
(22) Feller, D. *Chem. Phys. Lett.* **2000**, *322*, 543.
(23) Feller, D.; Dixon, D. A.; Nicholas, J. B. *J. Phys. Chem.* **2000**, *104*, 11414.
(24) Magnera, T. F.; David, D. E.; Stulik, D.; Orth, R. G.; Jonkman, H. T.; Michl, J. *J. Am. Chem. Soc.* **1989**, *111*, 5036.
(25) Dalleska, N. F.; Honma, K.; Sunderlin, L. S.; Armentrout, P. B. *J. Am. Chem. Soc.* **1994**, *116*, 3519.
(26) Rosi, M.; Bauschlicher, C. W. J. *J. Chem. Phys.* **1989**, *90*, 7264.
(27) Rosi, M.; Bauschlicher, C. W. J. *J. Chem. Phys.* **1990**, *92*, 1876.
(28) Bauschlicher, C. W., Jr.; Langhoff, S. R.; Partridge, H. *J. Chem. Phys.* **1990**, *94*, 2068.
(29) Feyereisen, M. W.; Feller, D.; Dixon, D. A. *J. Phys. Chem.* **1996**, *100*, 2993.
(30) Dixon, D. A.; Garza, J.; Hay, B. P.; Vargas, R. *J. Am. Chem. Soc.* **2000**, *122*, 4750.
(31) Peterson, K. A.; Xantheas, S. S.; Dixon, D. A.; Dunning, T. H., Jr. *J. Phys. Chem. A* **1998**, *102*, 2449.
(32) Liu, D.-J.; Oka, T.; Sears, T. J. *J. Chem. Phys.* **1986**, *84*, 1312.
(33) Pyykkö, P. *Chem. Rev.* **1988**, *88*, 563.
(34) Richtsmeier, S. C.; Dixon, D. A.; Gole, J. L. *J. Phys. Chem.* **1982**, *86*, 3937.
(35) Holland, P. M.; Castleman, A. W., Jr. *J. Am. Chem. Soc.* **1982**, *76*, 4195.